

Site-Selective Molecular Organization in Organic Heterostructures

Dimas G. de Oteyza,[†] Esther Barrena,^{*,†,‡} J. Oriol Ossó,[§] Stefan Sellner,[†] and Helmut Dosch^{†,‡}

Max-Planck-Institut für Metallforschung, Heisenbergstrasse 3, 70569 Stuttgart, Germany, Institut für Theoretische und Angewandte Physik, Universität Stuttgart, 70550 Stuttgart, Germany, and Institut de Ciència de Materials de Barcelona CSIC, 08193 Bellaterra, Spain

Received May 18, 2006

Revised Manuscript Received June 30, 2006

The high application potential of the so-called “plastic electronics” has sparked a worldwide research activity in the controlled and tailored growth of organic thin films.¹ Among the different explored materials, small aromatic molecules have been recognized as promising candidates for future applications, because they can be grown in films of high crystalline order, thus fulfilling one of the important requirements to obtain high charge carrier mobility.²

Because the charge transport within the organic film is directly dependent on its morphology and structure, a key challenge is the controlled growth of highly ordered organic layers. Up to now, the majority of the growth studies striving for this goal have been carried out on inorganic substrates,³ however, many electronic devices, such as organic light-emitting diodes (OLEDs), ambipolar transistors, or solar cells, rely on tailored p–n organic heterojunctions. Although numerous studies have been devoted to the performance of devices based on p–n organic heterojunctions, there are rather few structural studies addressing this important issue.⁴

* Corresponding author. Phone: +49 711 6891846. E-mail: barrena@mf.mpg.de.

[†] Max-Planck-Institut.

[‡] Universität Stuttgart.

[§] CSIC.

- (1) (a) Forrest, S. R. *Nature* **2004**, *428*, 911. (b) Kelley, T. W.; Baude, P. F.; Gerlach, C.; Ender, D. E.; Muyres, D.; Haase, M. A.; Vogel, D. E.; Theiss, S. D. *Chem. Mater.* **2004**, *16*, 4413.
- (2) (a) Dimitrakopoulos, C. D.; Malenfant, P. R. L. *Adv. Mater.* **2002**, *14*, 99. (b) Peumans, P.; Uchida, S.; Forrest, S. R. *Nature* **2003**, *425*, 158. (c) Newman, C. R.; Frisbie, C. D.; da Silva Filho, D. A.; Brédas, J.-L.; Ewbank, P. C.; Mann, K. R. *Chem. Mater.* **2004**, *16*, 4436. (d) Horowitz, G. *J. Mater. Res.* **2004**, *19*, 1946.
- (3) (a) Koma, A. *Prog. Cryst. Growth* **1995**, *30*, 129. (b) Forrest, S. R. *Chem. Rev.* **1997**, *97*, 1793. (c) Witte, G.; Wöll, C. *J. Mater. Res.* **2004**, *19*, 1889.
- (4) (a) Yang, F.; Shtein, M.; Forrest, S. R. *Nat. Mater.* **2005**, *4*, 37. (b) Kim, Y.; Cook, S.; Tuladhar, S. M.; Choulis, S. A.; Nelson, J.; Durrant, J. R.; Bradley, D. D. C.; Giles, M.; McCulloch, I.; Ha, C.-S.; Ree, M. *Nat. Mater.* **2006**, *5*, 197. (c) So, F. F.; Forrest, S. R.; Shi, Y. Q.; Steier, W. H. *Appl. Phys. Lett.* **1990**, *56*, 674 (13) Hoshino, A.; Isoda, S.; Kobayashi, T. *J. Cryst. Growth* **1991**, *115*, 826. (d) Akimichi, H.; Inoshita, T.; Hotta, S.; Noge, H.; Sakaki, H. *Appl. Phys. Lett.* **1993**, *63*, 3158. (e) Anderson, M. L.; Williams, V. S.; Schuerlein, T. J.; Collins, G. E.; England, C. D.; Chau, L.-K.; Lee, P. A.; Nebesny, K. W.; Armstrong, N. R. *Surf. Sci.* **1994**, *307–309*, 551. (f) Schuerlein, T. J.; Armstrong, N. R. *J. Vac. Sci. Technol., A* **1994**, *12*, 1992. (g) Forrest, S. R.; Burrows, P. E.; Haskal, E. I.; So, F. F. *Phys. Rev. B* **1994**, *49*, 11309. (h) Heutz, S.; Cloots, R.; Jones, T. S. *Appl. Phys. Lett.* **2000**, *77*, 3938. (i) Sellam, F.; Schmitz-Hübsch, T.; Toerker, M.; Mannsfeld, S.; Proehl, H.; Fritz, T.; Leo, K.; Simpson, C.; Müllen, K. *Surf. Sci.* **2001**, *478*, 113. (j) Heutz, S.; Jones, T. S. *J. Appl. Phys.* **2002**, *92*, 3039. (k) Yim, S.; Heutz, S.; Jones, T. S. *Phys. Rev. B* **2003**, *67*, 165308.

In turn, our present-day knowledge on the physical principles of the growth of organic heterostructures is still very poor.

In this communication we consider organic heterostructures based on fluorinated copper–phthalocyanines (F₁₆CuPc) and pentacene. F₁₆CuPc is one of the few air stable organic semiconductors showing n-type behavior,⁵ while pentacene (C₂₂H₁₄) shows preferentially p-type behavior and is characterized by its high charge carrier mobility. Combining in situ X-ray diffraction and atomic force microscopy (AFM) measurements we have obtained detailed insight into the microscopic processes which take place during the growth of F₁₆CuPc onto pentacene.

For the X-ray measurements, performed at the beamline ID-3 in the ESRF (Grenoble) with a wavelength of $\lambda = 0.72316 \text{ \AA}$, a pentacene film with nominal coverage of 130 \AA has been deposited at room temperature and a growth rate of 4 $\text{\AA}/\text{min}$ onto an ultrasonically cleaned Si(100) wafer covered by its native oxide. Afterward, F₁₆CuPc has been evaporated stepwise on the pentacene film, with coverages ranging between 15 and 225 \AA . One heterostructure consisting of 100 \AA F₁₆CuPc deposited on 752 \AA pentacene has been grown at a substrate temperature of 65 °C.

Figure 1 shows the scheme of the X-ray diffraction experiment and the experimental results obtained. The pristine pentacene film exhibits the well-known (001) and (002) Bragg reflections (Figure 1b) corresponding to a spacing of 15.6 \AA between molecular layers, as reported in previous studies for the thin-film structure.⁶

Upon room-temperature deposition of F₁₆CuPc (Figure 1b), the X-ray data reveal the growth of the expected standing-up structure (called the *s*-structure in the following). Because the F₁₆CuPc *s*-structure presents layers with a height of 14.3 \AA ,⁷ which is essentially the same as the layer height of the pentacene thin-film structure, the associated (001) and (002) Bragg peaks (which are broadened in the q_z direction by the thin-film geometry) almost coincide for both materials. Consequently, the growth of the F₁₆CuPc *s*-structure gives rise to a characteristic increase of the (001) and (002) reflections, accompanied by a slight shift to higher q_z -values (see inset in Figure 1b).

Most interestingly, we also observe the development of a new F₁₆CuPc-related Bragg reflection at $q_z = 2.0011 \text{ \AA}^{-1}$, corresponding to a molecular distance of 3.14 \AA . Because this spacing is identical with the intermolecular distance of cofacially oriented molecules, this observation gives a clear evidence for the growth of a new structure of F₁₆CuPc molecules which lie flat on the pentacene surface (called the

(5) Bao, Z.; Lovinger, A. J.; Brown, J. *Am. Chem. Soc.* **1998**, *120*, 207.

(6) (a) Dimitrakopoulos, C. D.; Brown, A. R.; Pomp, A. *J. Appl. Phys.* **1996**, *80*, 2501. (b) Ruiz, R.; Mayer, A. C.; Malliaras, G. G.; Nickel, B.; Scoles, G.; Kazimirov, A.; Kim, H.; Headrick, R. L.; Islam, Z. *Appl. Phys. Lett.* **2004**, *85*, 4926. (c) Mattheus, C. C.; Dros, A. B.; Baas, J.; Oostergetel, G. T.; Meetsma, A.; de Boer, J. L.; Palstra, T. T. M. *Synth. Met.* **2003**, *138*, 475.

(7) (a) de Oteyza, D. G.; Barrena, E.; Ossó, J. O.; Dosch, H.; Meyer, S.; Pflaum, J. *Appl. Phys. Lett.* **2005**, *87*, 183504. (b) Ossó, J. O.; Schreiber, F.; Alonso, M. I.; Garriga, M.; Barrena, E.; Dosch, H. *Org. Electron.* **2004**, *5*, 135.

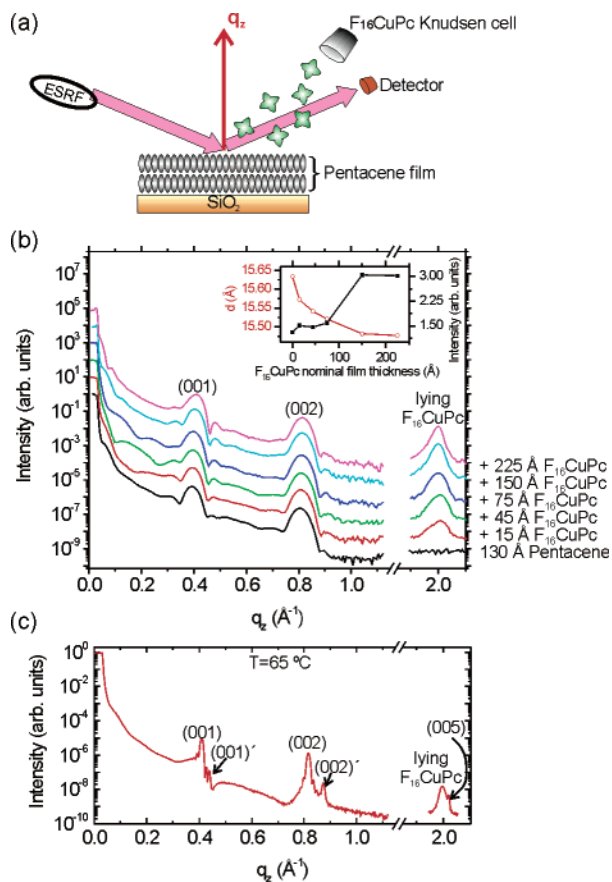


Figure 1. (a) Schematic representation of the in situ X-ray diffraction experiment. (b) Evolution of the specular X-ray diffraction data of a 130 Å thick pentacene film upon subsequent deposition of F₁₆CuPc. The inset represents the evolution of the spacing (open symbols) and integrated intensity (filled symbols) obtained from fits to the (002) Bragg reflection. (c) Specular X-ray diffraction data of a heterostructure of 100 Å F₁₆CuPc on 75 Å pentacene grown at a substrate temperature of 65 °C. The Bragg peaks arising from the pentacene bulk phase are labeled with a prime symbol.

l-structure in the following). The associated mosaicity is very small (0.017°) and close to that of the underlying pentacene structure (0.015°), implying an extremely good alignment of these crystallites with respect to the pentacene surface. The coexistent growth of F₁₆CuPc in the *s*- and *l*-structures is also observed at the organic heterostructure grown at 65 °C (Figure 1c). Thus, the emergence of the new *l*-structure is most likely not a kinetic phenomenon⁸ but rather induced by specific morphological details of the underlying pentacene substrate.⁹

To further explore which morphological features are responsible for these two competing F₁₆CuPc growth modes, we have performed extensive AFM experiments. Figure 2a shows a topographic image of a pentacene film grown on SiO₂ with a nominal thickness of 40 Å, measured with a commercial Omicron atomic force microscope in contact mode under ultrahigh vacuum conditions and without breaking the vacuum upon transfer to and from the growth

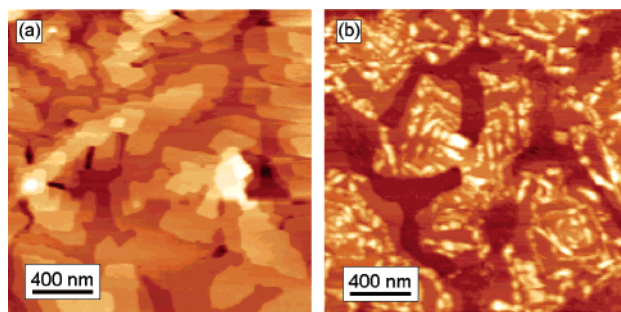


Figure 2. Topographic AFM image (a) of a 40 Å thick pentacene film and (b) upon deposition of 60 Å F₁₆CuPc onto the same sample.

chamber. The image reveals the layered pentacene structure with monomolecular steps of ~15 Å. The same film upon deposition of 60 Å of F₁₆CuPc is shown in Figure 2b.¹⁰ The F₁₆CuPc growth results in an interesting morphology consisting of islands of small lateral dimensions (50–100 nm) which decorate the pentacene steps. Their heights vary between 90 and 170 Å and, as we will discuss below, are associated with the F₁₆CuPc *l*-structure.

As a result of the similar heights of F₁₆CuPc and pentacene monomolecular layers ($h_{\text{F}_{16}\text{CuPc}} = 14.3$ Å vs $h_{\text{pentacene}} = 15.6$ Å), the identification of the F₁₆CuPc *s*-structure in the topography images is rather difficult. We have employed the phase-shift signal, which is sensitive to the material-dependent dissipative processes related to the tip-sample interactions.¹¹ This provides us with a tool to distinguish between F₁₆CuPc *s*-structure and uncovered pentacene at samples with F₁₆CuPc submonolayer coverage. This is illustrated in Figure 3, depicting the topography (Figure 3a) and phase-shift signal (Figure 3b) of a sample with 8 Å (0.56 monolayers) F₁₆CuPc deposited onto 35 Å of pentacene. The phase shift of the tapping mode (Figure 3b) discloses the growth of the F₁₆CuPc *s*-structure (darker) on top of the pentacene terraces (uncovered pentacene appears lighter). The crystallites of the F₁₆CuPc *l*-structure are better distinguished in the topography than in the phase images, because the phase-shift contrast is just dominated by large changes at the island edges caused by the limited response speed of the feedback to abrupt topographic changes.¹¹ The correlation between topography and phase-shift signal is further clarified in Figure 3c, which shows a cross section for both signals on the same area (marked on the respective images) together with the deduced distribution of the different materials and structures which give rise to the observed topographic features. Interestingly, the heights of the F₁₆CuPc *l*-structure crystallites show no apparent correlation with the pentacene terrace size or with the coverage of F₁₆CuPc *s*-structure, suggesting that surface diffusion does not play a dominant role on their growth.

The combined X-ray diffraction and AFM study reveals the competing formation of two F₁₆CuPc structures: the *s*-structure grows on top of the pentacene terraces, while the *l*-structure develops along the pentacene step edges

(8) Dürr, A. C.; Nickel, B.; Sharma, V.; Täffner, U.; Dosch, H. *Thin Solid Films* **2006**, *503*, 127.

(9) For this higher substrate temperature (and due to the higher pentacene thickness), the coexistent formation of pentacene thin-film and bulk phases takes place (see ref 6), as evidenced by the emergence of additional Bragg reflections corresponding to a layer spacing of 14.5 Å.

(10) The images have been obtained with a commercial Nanotec scanning probe microscope in tapping mode (under ambient conditions) because in contact mode the F₁₆CuPc molecules were swept by the AFM tip even at minimized applied loads.

(11) Garcia, R.; Perez, R. *Surf. Sci. Rep.* **2002**, *47*, 197.

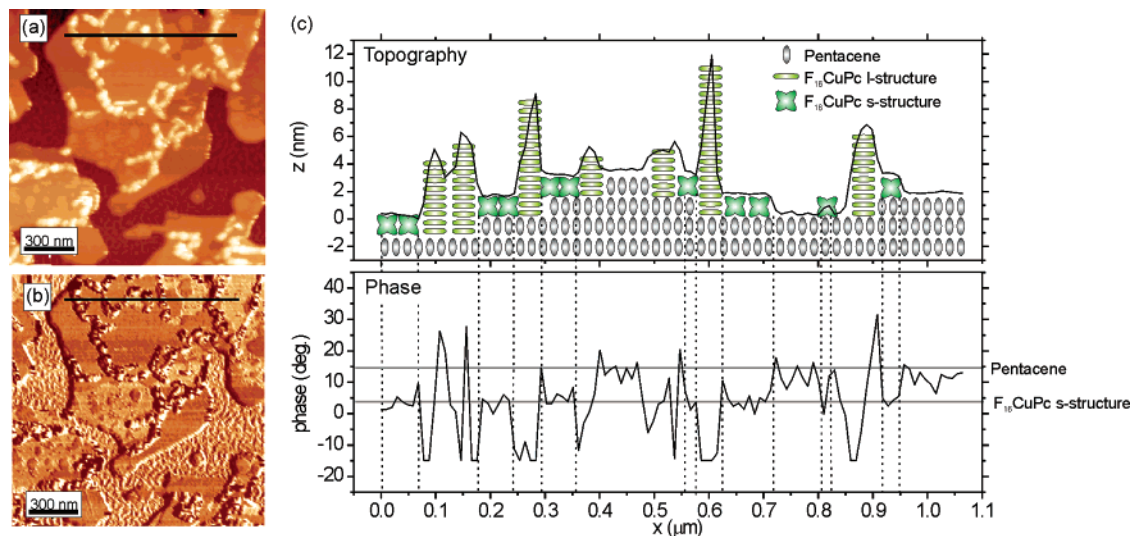


Figure 3. (a) Topographic tapping mode AFM image of 8 Å $F_{16}\text{CuPc}$ grown on 35 Å pentacene. (b) Phase-shift image obtained simultaneously with image a. (c) Topographic (top) and phase-signal (bottom) profiles of the same region (as marked on images a and b), together with a schematic representation of the different molecules and structures forming the observed topographic features. The horizontal lines in the phase profile mark the mean values for the pentacene and $F_{16}\text{CuPc}$ s -structure. The vertical lines help with the correlation of both signals.

(Figure 3c). Note here that the pentacene terraces expose the (001) facets, which correspond to the lowest energy pentacene planes.¹² On top of this weakly interacting surface, $F_{16}\text{CuPc}$ is able to adopt its energetically preferred standing configuration, similarly to that observed for the $F_{16}\text{CuPc}$ growth on other weakly interacting surfaces such as SiO_2 ,⁷ Al_2O_3 ,¹³ OTMS,^{7a} or polymers.¹⁴ However, for $F_{16}\text{CuPc}$ molecules at pentacene steps, the different energetic and electronic environment at the step edges favors the orientation of the phthalocyanines with its molecular plane parallel to the surface. The fact that similar results are obtained at higher substrate temperature (65 °C) implies a rather strong interaction ($\gg k_B T$) of $F_{16}\text{CuPc}$ with pentacene at the steps. Once an initial nucleus of molecules in the l -structure is formed,

a rapid vertical growth of this crystallographic face occurs simply as a result of the strong interaction between π orbitals, favoring the cofacial vertical stacking and promoting the observed morphology of narrow and high crystallites.

These results clearly demonstrate that the intrinsic anisotropy of the organic systems gives rise to complex growth scenarios which are not covered by current growth theories. Because the steps of the underlying pentacene catalyze the growth of the $F_{16}\text{CuPc}$ l -structure, this may be used for controlling the morphology and structure of organic films by the use of vicinal organic templates.

Acknowledgment. The authors thank R.G. Della Valle for fruitful discussions and J. Pflaum and S. Hirschman for purifying the molecules. The authors acknowledge the ESRF for provision of synchrotron radiation facilities and H. Kim for assistance in using the beamline ID-3.

(12) Northrup, J. E.; Tiago, M. L.; Louie, S. G. *Phys. Rev. B* **2002**, *66*, 121404.

(13) (a) Ossó, J. O.; Schreiber, F.; Kruppa, V.; Dosch, H.; Garriga, M.; Alonso, M. I. Cerdeira, F. *Adv. Funct. Mater.* **2002**, *12*, 455. (b) Barrera, E.; Ossó, J. O.; Schreiber, F.; Garriga, M.; Alonso, M. I.; Dosch, H. *J. Mater. Res.* **2004**, *19*, 2061.

(14) Oh, Y.; Pyo, S.; Yi, M. H.; Kwon, S.-K. *Org. Electron.* **2006**, *7*, 77.